

Axicon lens-based cone shell configuration for depth-sensitive fluorescence measurements in turbid media

Yi Hong Ong and Quan Liu*

School of Chemical and Biomedical Engineering, Nanyang Technological University, 70 Nanyang Drive, Singapore 637457

*Corresponding author: quanliu@ntu.edu.sg

Received April 11, 2013; revised May 27, 2013; accepted June 6, 2013;
posted June 25, 2013 (Doc. ID 188650); published July 19, 2013

We have developed a novel noncontact setup to implement a cone shell illumination and detection configuration using axicon lenses for depth-sensitive fluorescence measurements. The setup was demonstrated experimentally to be capable of detecting fluorescence from a two-layered turbid agar phantom with a larger sensitivity to the deep layer and a larger range of sensitivity to either layer than a conventional cone configuration implemented by a microscope objective lens. Furthermore, the axicon lens-based setup eliminates the need of moving the objective lens up or down to achieve depth-sensitive measurements, which effectively improves the consistency of optical coupling and thus would be preferred in a clinical setting. © 2013 Optical Society of America

OCIS codes: (110.0113) Imaging through turbid media; (110.2945) Illumination design; (170.2520) Fluorescence microscopy.

<http://dx.doi.org/10.1364/OL.38.002647>

Ultraviolet–visible fluorescence spectroscopy has been widely explored in the detection of precancers in human epithelial tissues. Vital diagnostic information about morphological and biochemical changes can be extracted from various fluorophores present in epithelial tissues. However, the distribution of endogenous fluorophores is affected by the progression of the disease state and various other factors [1]. Hence, a depth-sensitive probe that can measure fluorescence spectra as a function of depth will enhance the diagnostic performance of this technique. Currently, depth-sensitive fluorescence measurements can be achieved in two approaches, namely the fiber optic-based contact setup and the lens-based noncontact setup. Fiber optic setups achieve depth-sensitive measurements by varying the source-detector separation [2], aperture diameter [3], and/or angle of illumination and collection fibers [1]. Lens-based setups [4] use a single lens or a combination of lenses to achieve a cone configuration, in which both the excitation and emission volumes would form light cones in an optically transparent medium. One weakness of this setup is the limited sensitivity to fluorescence originating from sub-surface layers due to the contribution from shallower layers in a layered structure such as epithelial tissues. A cone shell configuration has been previously proposed [4] in a numerical study to yield larger depth sensitivity to deep layers than the cone configuration in diffuse reflectance measurements from a numerical model of squamous cell carcinoma. However, the cone shell configuration requires the alteration of distance between the imaging lens and the tissue sample in order to achieve depth-sensitive measurements, which induces uncertainty in optical coupling and great inconvenience in clinical measurements.

In this study, we introduce a new cone shell illumination and collection configuration based on the combination of multiple axicon lenses to overcome the weaknesses of the cone configuration in limited depth sensitivity to deep layers as well as to eliminate the need of altering the lens–sample distance in depth-sensitive measurements. The

same configuration could also be applied in other optical measurements such as diffuse reflectance or Raman measurements.

We constructed a fluorescence probe with the cone illumination and detection configuration as shown in Fig. 1(a). The probe was coupled to a diode laser (iFlex-2000, Point Source Ltd., Hamble, UK) through a single-mode fiber with a maximum output power of 30 mW at 405 nm. The output laser light was collimated using a convex lens ($f = 50.0$ mm) to achieve a beam diameter of 6 mm before passing through a 405 nm band-pass filter and was deflected by a dichroic mirror toward a microscope objective lens (10 \times , NA = 0.25). The fluorescence signal was collected through the same objective lens, which then passed through a long pass filter before being focused onto the tip of a collection fiber with a core diameter of 400 μ m and an NA of 0.22. In the cone shell configuration as shown in Fig. 1(b), a collimated laser beam of 3 mm in diameter was passed through a pair of axicon lenses (Altechna Co. Ltd., Vilnius, Lithuania), namely axicon 1 and axicon 2, with an identical apex angle (140 $^\circ$) to create a donut-shape laser ring. The laser ring was then focused onto the sample by the third axicon lens, namely axicon 3, with an apex angle of 110 $^\circ$, forming the cone shell geometry. The fluorescence signal

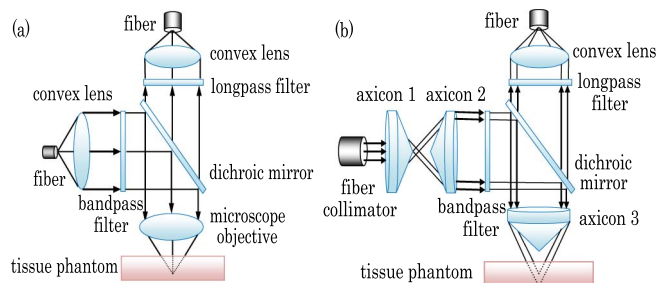


Fig. 1. Schematic diagram of (a) the cone illumination and detection configuration based on a microscope objective lens and (b) the cone shell configuration based on the combination of axicon lenses.

will come back through axicon 3 and a long pass filter and then be focused onto the same collection fiber as in the cone configuration. The fluorescence signals transmitted by the collection fiber in both configurations were coupled to a Czerny–Turner-type spectrograph (Shamrock 303, Andor Technology, Belfast, UK) equipped with a holographic grating (1200 groove/mm) and a research-grade CCD (DU920P-BR-DD, Andor Technology, Belfast, UK), which yields a spectral resolution of 0.1 nm. The integration time for this experiment was always 1 s. The laser powers on the sample were measured to be 10 and 7 mW for the cone and cone shell configurations, respectively.

A two-layered agar phantom was fabricated to mimic the stratified structure of human skin according to the recipe and procedure published in an earlier report [5]. The thickness of the top layer was 1 mm, and the thickness of the bottom layer was 10 mm, whereas the lateral dimension of both layers was made greater than 30 mm in diameter to represent a semi-infinite medium. Two different endogenous fluorophores, flavin adenine dinucleotide (FAD) and protoporphyrin IX (PpIX), were added to the top and bottom layers of the phantom to discriminate fluorescence from the two layers, which is facilitated by the nonoverlapping emission peaks of FAD and PpIX at 525 and 630 nm, respectively. A concentration of 33.2 μM for FAD and a concentration of 32.3 μM for PpIX were used so that the intensities of both emission peaks fell within the same order of magnitude for the ease of data analysis. A piece of plastic wrap was placed between the two layers to prevent the diffusion of fluorophores between layers. Intralipid 20% (Fresenius Kabi, Bad Homburg, Germany) was added into each layer at a different concentration to mimic the light-scattering properties of the epidermis and dermis so that the reduced scattering coefficient, μ'_s , matched the published value at 525 nm [6]. The optical properties of the phantom (μ'_s and μ_a) at the excitation wavelength (405 nm) and peak emission wavelengths of PpIX (630 nm) were estimated by extrapolating the optical properties of intralipid at the concentration reported [7] to obtain those for the concentration of intralipid used in our experiment. Such extrapolation assumed that μ'_s and μ_a are proportional to the concentration of intralipid. The optical properties of each layer of the phantom at the excitation and emission wavelengths were listed in Table 1.

A range of apparent focal depths were achieved by varying the lens–sample distance in the cone configuration as shown in Fig. 1(a). A similar focal depth range was achieved by varying the distance between axicon lenses 1 and 2 in the cone shell configuration as shown in Fig. 1(b), which minimized the variation in optical coupling. The targeted focal depths inside tissue phantoms were estimated by correcting for the refractive index mismatch between the phantom and air as described by Overall [8] based on a refractive index of 1.364 for the phantom and a refractive index of 1 for air at 405 nm [9].

Figure 2 shows the fluorescence spectra measured at a range of targeted focal depths from the two-layered phantom using the cone shell configuration as shown in Fig. 1(b). FAD fluorescence peak intensity (at 525 nm) gradually increases from the surface (0 mm) until reaching a maximum at a depth of 1.3 mm and decreases

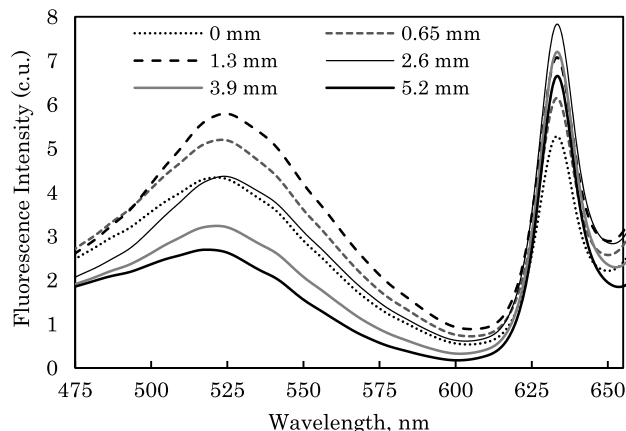


Fig. 2. Fluorescence spectra measured using the cone shell configuration from the two-layered phantom at a range of targeted focal depths corrected for refractive index mismatch. The abbreviation “c.u.” refers to the calibrated unit.

noticeably from 1.3 to 5.2 mm. PpIX fluorescence peak intensity (at 630 nm) also increases as the focal depth increases from 0 to 2.6 mm and decreases as the focal depth increases further. This trend, in which the peak intensity increased to the maximum and then decreased, can be attributed to two factors. The first factor is that the length of the line focus formed by axicon 3 was around 1.7 mm, which caused half of the line focus to be still in air when the focal depth was zero. The second factor is light attenuation due to the significant increase in light path length that causes the detected fluorescence signal to decrease. While the first factor prevented the maximum from occurring at zero focal depth, the second factor pushed the maximum toward the surface. The combination of two factors implied that the maximum corresponding to each layer had to occur in the middle of the layer as observed in Fig. 2. This has been consistently observed when we performed a series of depth-sensitive measurements in a homogenous sample. Fluorescence intensities corresponding to the top and bottom layers reached maxima at different focal depths, which demonstrated that the cone shell configuration using axicon lenses was capable

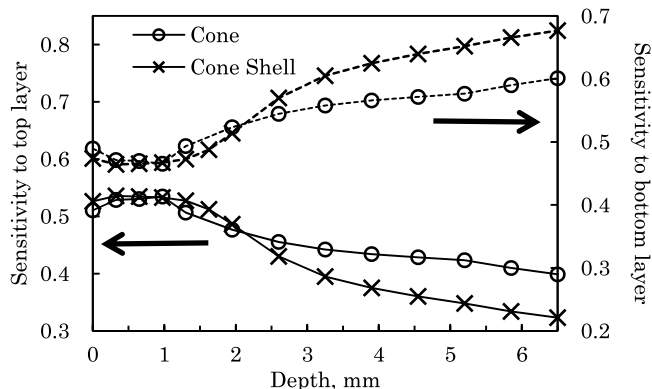


Fig. 3. Sensitivity to the top and bottom layers as a function of the targeted depth of focus beneath the phantom surface, which has been corrected for refractive index mismatch between the sample and air. “O” refers to the cone configuration; “x” refers to the cone shell configuration. The solid line and dashed line indicate the sensitivities to the top layer and the bottom layer, respectively.

Table 1. Optical Properties (μ'_s [cm^{-1}] and μ_a [cm^{-1}]) of the Top and Bottom Layers for Tissue Phantom at the Excitation Wavelength and at the Peak Emission Wavelengths of FAD and PpIX. μ'_s Refers to the Reduced Scattering Coefficient; μ_a Refers to the Absorption Coefficient

Layer	Wavelength (nm)		
	405 (Excitation)	525 (FAD)	630 (PpIX)
Top	80, 0.09	63, 0.03	55, 0.10
Bottom	51, 0.06	40, 0.02	35, 0.06

of performing depth-sensitive fluorescence measurements without altering the lens-sample distance. To compare the sensitivity improvement achieved by this approach, we have computed the sensitivity of measured fluorescence to the top and bottom layer as a function of the targeted depth for both the cone and cone shell configurations as follows. First, each raw FAD peak intensity measured at every depth was divided by the maximum among these intensities to obtain normalized FAD intensities. Similarly, each raw PpIX peak intensity measured at every depth was divided by the maximum among these intensities to obtain normalized PpIX intensities. Then, the sensitivity to the top layer at each depth was calculated by dividing the normalized FAD intensity at this depth by the sum of normalized FAD and PpIX fluorescence intensities at this depth. Similarly, the sensitivity to the bottom layer at each depth was calculated by dividing the normalized PpIX intensity at this depth by the sum of normalized FAD and PpIX fluorescence intensities at this depth.

From Fig. 3, it can be seen that the maximum sensitivities of both the cone and cone shell configuration to the top layer are around 0.53 but the maximum location of the cone configuration has a narrower peak at 0.98 mm, close to the actual thickness of the top layer. This can be explained by the difference in the focal spot size between two configurations. The microscope objective lens in the cone configuration formed a tiny focal spot of 20.9 μm in diameter, which was much smaller than the top layer thickness. In contrast, the axicon lens formed an elongated focal line of around 1.7 mm in the axial dimension, which is estimated using the Pythagoras theorem given that the thickness of the laser ring incident on axicon 3 was measured to be 0.8 mm. Therefore the depth resolution of the cone configuration is superior to that of the cone shell configuration. The minimum sensitivity to the top layer for the cone shell configuration, which is 0.32 at a focal depth of 6.5 mm, is lower than that for the cone configuration, which is 0.4 at the same

focal depth. Therefore the range of the sensitivity to the top layer achieved with the cone shell configuration is larger than that with the cone configuration. The maximum sensitivity to the bottom layer for the cone configuration, which is 0.60 at a focal depth of 6.5 mm, is considerably lower than that for the cone shell configuration, which is 0.68 at the same focal depth. It is noted that this depth corresponds to the minimum sensitivity to the top layer. This observation can be attributed to the high possibility that the cone shell configuration effectively reduced the illumination volume near the surface when focusing on a deep layer due to the absence of the light core in the volume. As a consequence, the contribution of fluorescence from the top layer was effectively weakened, which resulted in a higher maximum sensitivity to the bottom layer. Moreover, the range of the sensitivity to the bottom layer achieved with the cone shell configuration is also larger than that with the cone configuration.

In this Letter, we have experimentally demonstrated that a cone shell configuration involving multiple axicon lenses detects fluorescence with a higher sensitivity to the bottom layer and a larger range of sensitivity to either the top or the bottom layer in a two-layered tissue phantom mimicking human skin. Furthermore, these can be achieved without altering the distance between the imaging lens and the sample, which minimizes inconsistency in optical coupling and brings great convenience in potential clinical measurements.

The authors gratefully acknowledge financial support from the New Investigator Grant (Project No. NMRC/NIG/1044/2011) funded by the National Medical Research Council (NMRC) and a Tier 1 grant and Tier 2 grant funded by the Ministry of Education in Singapore (Grant Nos. RG47/09 and MOE 2010-T2-1-049).

References

1. Q. Liu and N. Ramanujam, *Opt. Lett.* **29**, 2034 (2004).
2. T. J. Pfefer, L. S. Matchette, A. M. Ross, and M. N. Ediger, *Opt. Lett.* **28**, 120 (2003).
3. Q. Liu and N. Ramanujam, *Opt. Lett.* **27**, 104 (2002).
4. C. G. Zhu and Q. Liu, *Opt. Express* **20**, 29807 (2012).
5. R. Cubeddu, A. Pifferi, P. Taroni, A. Torricelli, and G. Valentini, *Phys. Med. Biol.* **42**, 1971 (1997).
6. E. Salomatina, B. Jiang, J. Novak, and A. N. Yaroslavsky, *J. Biomed. Opt.* **11**, 064026 (2006).
7. R. Michels, F. Foschum, and A. Kienle, *Opt. Express* **16**, 5907 (2008).
8. N. Everall, *Appl. Spectrosc.* **54**, 773 (2000).
9. H. F. Ding, J. Q. Lu, K. M. Jacobs, and X. H. Hu, *J. Opt. Soc. Am.* **22**, 1151 (2005).